A Repurposed Duo: Empagliflozin-Metformin Triggers a Metabolic Crisis in Cervical Cancer by Disrupting the Acyl-CoA/CoA Ratio via Dual Inhibition of PPAT and CPT1A

Ali Muafaq Said[1], Ayat Ali Salih[2], Mohammed Abdulridha Obid[1], Azal Hamoody Jumaa[3] and Youssef Shakuri Yasin[4,*]

[1]*Al-Amarah University College, Misan, Iraq*

[2]*Department of Biology, College of Education for Pure Sciences, Tikrit University, Iraq*

[3]*Bilad Alrafidain University, Iraq*

[4]*Iraqi National Cancer Research Center/the University of Baghdad, Iraq*

Abstract: *Objective*: This study aimed to assess the cytotoxic, selective, and synergistic effects of an Empagliflozin-Metformin mixture against HeLa cervical cancer cells and to investigate its underlying mechanism of action, especially through metabolic disruption.

Materials and Methods: The cytotoxic effects of Empagliflozin, Metformin, carboplatin, and their mixture were evaluated in HeLa and human foreskin fibroblast (HFF) cells using the MTT assay at 24 and 72 hours. The Combination Index (CI) and Dose Reduction Index (DRI) were calculated to assess drug interactions. Metabolic disruption was analyzed by measuring the intracellular Acyl-CoA/CoA ratio. Molecular docking simulations were performed to predict binding affinities for key metabolic enzymes, Phosphopantetheine Adenylyl Transferase (PPAT) and Carnitine Palmitoyl Transferase 1A (CPT1A).

Results: The mixture showed clear, time-dependent cytotoxic effects on HeLa cells, with an IC_{50} of 207.5 µg/ml at 72 hours, which is significantly lower than the IC_{50} values of either agent alone. The combination exhibited high selectivity toward malignant cells, with a Selectivity Index of over 4.82, and demonstrated strong synergistic interactions, as indicated by a combination index (CI) of less than 1.0. Additionally, a dose-dependent increase in the Acyl-CoA/CoA ratio was observed (5.02 ± 0.41 at 1000 µg/ml), indicating considerable metabolic stress. Molecular docking analyses showed strong binding affinities for both drugs to PPAT and CPT1A, with docking scores of -7.4 and -8.7 kcal/mol for Empagliflozin and -5.2 and -5.1 kcal/mol for metformin, respectively. Suggesting dual inhibitory effects on CoA biosynthesis and fatty acid oxidation.

Conclusion: This study identifies the combination of Empagliflozin and Metformin as a promising candidate for repurposing as a therapeutic agent in cervical cancer. The therapeutic potential is supported by the well-characterized pharmacokinetics and established safety profiles of both agents, which are extensively used in the management of diabetes. The observed synergistic effect facilitates effective cytotoxicity at lower concentrations, thereby potentially minimizing adverse effects and enhancing the translational prospects of this metabolic-targeting strategy in clinical oncology trials.

Keywords: Empagliflozin, Metformin, Cervical cancer, Metabolic disruption, Synergistic, cytotoxicity, Drug repurposing.

1. INTRODUCTION

Cervical carcinoma remains a major public health issue worldwide, ranking as the fourth most common cancer and the leading cause of cancer-related death among women [1]. While high-income countries have experienced reductions in HPV-related diseases due to widespread vaccination and screening efforts, the disease primarily affects women in low- and middle-income countries where access to preventive healthcare is limited [2]. In patients with advanced, recurrent, or metastatic disease, treatment mainly involves platinum-based chemotherapy agents like cisplatin, often combined with additional drugs such as 5-fluorouracil (5-FU) [3].

However, the clinical usefulness of these regimens is often limited by the development of acquired chemoresistance and the occurrence of severe, dose-limiting systemic toxicities, both of which significantly decrease patients' quality of life [4].

Chemotherapy resistance remains a major challenge in treating cervical cancer, often leading to relapse and poor outcomes. To address this, drug repurposing has emerged as a promising strategy, leveraging existing non-cancer drugs with established safety profiles to enhance cancer targeting. This approach accelerates the process of bringing treatments to patients and reduces development costs.

*Address correspondence to this author at the Iraqi National Cancer Research Center/the University of Baghdad, Iraq; E-mail: dryoussef@bauc14.edu.iq

ISSN: 1929-2260 / E-ISSN: 1929-2279/25

For example, antidiabetic medications are currently being explored [5-13].

An example of an anti-diabetic agent with potential anti-cancer effects is the sodium-glucose cotransporter 2 (SGLT2) inhibitor class. The recent approval of these drugs for the management of type 2 diabetes has sparked increased research interest due to their potential off-target anticancer properties. Preclinical studies suggest that, beyond controlling blood glucose, they may also slow tumor growth and induce cell death by interfering with cellular glucose metabolic pathways, such as the Warburg effect, which are often exploited by cancer cells [14, 15].

Similarly, metformin, a widely prescribed biguanide for the management of type 2 diabetes mellitus, has garnered significant attention for its potential application as an anticancer agent. In addition to its glucose-lowering effects, metformin exhibits direct antitumor properties, primarily mediated through the activation of AMP-activated protein kinase (AMPK). This activation inhibits the mammalian target of rapamycin (mTOR) pathway, a critical regulator of cellular growth and proliferation that is frequently hyperactive in various cancers [16, 17]. Evidence suggests that metformin induces cell cycle arrest and apoptosis across various cancer models. Its capacity to selectively target cancer cell metabolism, particularly under hypoxic conditions, positions it as a promising agent for combination therapy. This approach aims to circumvent chemoresistance and reduce treatment-related toxicity [18, 19].

To achieve effective cancer treatment, various therapeutic targets have been proposed, among which cancer cell metabolic pathways are of particular interest. These cells undergo extensive metabolic reprogramming to sustain their rapid proliferation and survival, representing a hallmark of malignancy that extends beyond the classical Warburg effect [20]. Central to this metabolic reprogramming is the dynamic equilibrium of coenzyme A (CoA) species, with particular emphasis on the acyl-CoA to free CoA (CoASH) ratio [21]. This equilibrium is crucial for the preservation of fundamental cellular functions, such as lipid biosynthesis, energy generation via β-oxidation, and the tricarboxylic acid (TCA) cycle. Central to this metabolic adaptation is the dynamic balance of coenzyme A (CoA) species, particularly the acyl-CoA to free CoA (CoASH) ratio [22].

This balance is crucial for maintaining essential cellular processes, including lipid biosynthesis, energy generation through β-oxidation, and the tricarboxylic acid (TCA) cycle. In oncological contexts, disruption of the acyl-CoA/CoA ratio may indicate metabolic distress, as the accumulation of acyl-CoA esters can inhibit critical mitochondrial enzymes, such as α-ketoglutarate dehydrogenase, consequently impairing ATP synthesis and potentially inducing apoptotic cell death [22, 23].

Consequently, targeting the induction of a metabolic crisis by modulating the Coenzyme A (CoA) pool emerges as a promising therapeutic strategy in oncology. Enzymes integral to CoA metabolism, including Phosphopantetheine adenylyl transferase (PPAT), which catalyzes a rate-limiting step in CoA biosynthesis, and carnitine palmitoyl transferase 1A (CPT1A), the principal enzyme mediating mitochondrial fatty acid oxidation (FAO), are frequently overexpressed across diverse tumor types [24, 25]. Their increased expression is crucial for the metabolic changes that enable cancer cells to grow, survive, and resist chemotherapy [20, 26].

PPAT facilitates anabolic processes by supplying essential CoA required for lipid and amino acid biosynthesis. Concurrently, CPT1A enables cancer cells to use fatty acids as an alternative energy substrate, particularly under metabolic stress [27, 28].

While the individual anticancer effects of empagliflozin and metformin are well established, their combined capacity to induce a synergistic metabolic crisis in cervical cancer has not been thoroughly investigated. It is hypothesized that their simultaneous inhibition of PPAT and CPT1A more significantly disrupts the acyl-CoA/CoA ratio than either agent alone, presenting a potential mechanism-based repurposing approach to overcome chemoresistance with improved specificity.

Despite extensive prior research in this domain, limitations persist in fully elucidating the anticancer efficacy of combined Empagliflozin and Metformin therapy. Notably, questions remain regarding its capacity to elicit synergistic and selective cytotoxic effects against cervical carcinoma cells by modulating metabolic pathways involving key enzymes such as PPAT and CPT1A.

The current study aims to address existing research gaps by employing an innovative method to assess the anticancer potential of drug repurposing, specifically by combining empagliflozin and metformin for the treatment of cervical cancer. Additionally, a quantitative

evaluation of drug interactions was performed. Mechanistic insights were obtained by analyzing the Acyl-CoA/CoA ratio and by conducting in silico molecular docking studies that examined the binding affinities of key metabolic enzymes, including PPAT and CPT1A.

2. MATERIALS AND METHODS

2.1. Study Medication

Study medications, including Empagliflozin, Metformin, and Carboplatin, were obtained as raw materials from the Samarra Pharmaceutical Factory in Iraq. These compounds, along with their combined formulation, were diluted in Minimum Essential Medium (MEM) to achieve concentrations ranging from 0.1 to 1000 µg/mL. Specifically, in the combined formulation, Empagliflozin and Metformin were present at concentrations of 0.05 to 50 µg/mL, yielding a final concentration range of 0.1 to 1000 µg/mL.

2.2. Cytotoxicity Assay

The cytotoxicity of the study agents was assessed in the human cervical carcinoma cell line HeLa to evaluate the anticancer effects of Empagliflozin, Metformin, Carboplatin, and a combination of Empagliflozin and Metformin. They also investigated how the combination affects the normal human foreskin fibroblast cell line, which represents healthy, non-cancerous cells, to assess safety and potential drug interactions that could harm cell viability.

Furthermore, the cytotoxicity and safety profiles of these agents were evaluated by measuring cellular viability in both cancer and normal cells across a concentration range of 0.1-1000 µg/ml. The cell lines used in this study were obtained from the Tissue Culture Unit at ICCMGR.

2.2.1. Cell Lines

The study used two cell lines: a cancerous cell line, HeLa, derived from human cervical cancer tissue [29, 30]. The normal healthy cell line, represented by the HFF cell line, originates from normal human Foreskin Fibroblasts [31].

2.2.2. Tissue Culture Conditions

MEM media from US Biological (USA) was used to culture the cell line. The medium was supplemented with 10% (v/v) fetal bovine serum (FBS) from Capricorn Scientific (Germany), along with 100 IU/mL of penicillin and 100 µg/mL of streptomycin to prevent bacterial contamination. The cells were maintained in a humidified incubator at 37 °C during exponential growth [32].

2.2.3. Cytotoxicity Study

The MTT assay is a widely used colorimetric method for measuring cell metabolic activity. It works by enabling living cells to convert the tetrazolium salt MTT into insoluble purple formazan crystals, a process driven by mitochondrial dehydrogenase enzymes. Typically, cells are cultured in a 96-well plate and exposed to different concentrations of test compounds. After incubation, MTT is added to each well, and the plates are incubated again to allow reduction to occur. Viable cells facilitate the conversion of MTT into formazan, which is then dissolved in a solution. The absorbance of the resulting solution is measured at a specific wavelength with a spectrophotometer to evaluate cell viability.

There is a direct relationship between the number of viable cells and the amount of formazan produced. A reduction in formazan levels after treatment with the tested pharmaceuticals indicates cytotoxic effects, as evidenced by lower absorbance readings. The dose-response curve was used to determine the half-maximal inhibitory concentration (IC50), defined as the drug concentration that reduces cell viability by 50%. It is calculated using GraphPad Prism software (version 9.5.0, build 750) [33, 34].

Cells were cultured in 96-well microplates at 10,000 cells per well and incubated at 37°C for 24 hours until confluence. The MTT assay was used to assess the cytotoxic effects of Empagliflozin, Metformin, Carboplatin, and the combination of Empagliflozin and Metformin. Six replicate wells were used for each concentration. Cells were treated with various concentrations (0.1, 1, 10, 100, and 1000 µg/mL), with untreated controls serving as negative references. After 24 and 72 hours of treatment, 28 µL of MTT solution (2 mg/mL) was added to each well, and the plates were incubated for 3 h. Subsequently, 100 µL of DMSO was added to each well and incubated for an additional 15 minutes to dissolve the formazan crystals. Absorbance was measured at 570 nm using a microplate reader. The growth percentage was calculated using the following equation [35].

$$\text{Growth inhibition } \% = \frac{\text{optical density of control wells - optical denity of treated wells}}{\text{optical density of control wells}} * 100\%$$

2.3. Selective Toxicity Index

The selective toxicity index was used to evaluate the cytotoxic selectivity of the Empagliflozin–Metformin combination compared with Carboplatin in cancer cell lines after incubation for 24 and 72 hours. IC50 values were determined for both the combination and Carboplatin, and the selective cytotoxicity index was calculated using a mathematical formula based on cellular growth curves obtained from HeLa cells and normal human Foreskin Fibroblasts (HFF) [36], as the following mathematical equation

$$\text{Selective toxicity indes (SI)} = \frac{\text{IC50 of normal cell lines}}{\text{IC50 of cancer cell lines}}$$

When an SI score is above 1.0, it indicates that a drug can target tumor cells more effectively than it harms normal cells.

2.4. Mapping of drug Combinations

2.4.1. Combination Index- CI

Compusyn, a computational simulation tool, was employed to calculate the combination index (CI) scores. The primary objective of this analysis was to determine whether the mixture's constituents exhibited synergistic, additive, or antagonistic interactions. This assessment was conducted using concentration-effect curves that depict the percentage inhibition of cell proliferation across a range of drug concentrations at 24 and 72 hours post-treatment.

CI values below one show synergy, equal to 1 indicate additivity, and above 1 indicate antagonism. We used Compusyn software (Biosoft, Ferguson, MO) to determine the combination index USA) [37, 38].

2.4.2. Dose Reduction Index- DRI

Compusyn, a computational simulator, determined Dose Reduction Index (DRI) scores. The DRI score indicates the maximum reduction in the concentration of each drug in a mixture that preserves its cytotoxic effect.

When the DRI score exceeds 1, it signifies a favorable decrease in concentration. Conversely, a score below 1 indicates an unfavorable reduction. The DRI analysis was conducted using Compusyn software (Biosoft, Ferguson, MO, USA) [377, 38].

2.5. Morphological Assessment

After 72 hours of treatment with the test compounds, morphological changes in HeLa cells were observed and photographed under an inverted light microscope.

2.6. Quantification of the Acyl-CoA/CoA Ratio

The study aims to investigate the impact of the empagliflozin–metformin combination on metabolic processes in cervical cancer cells, with the goal of elucidating the mechanisms underlying their combined cytotoxicity and potential synergistic effects.

The intracellular Acyl-CoA to CoA ratio was quantified. This ratio serves as a critical marker of metabolic stress and dysregulation, reflecting the equilibrium between activated fatty acids—substrates for oxidation and synthesis—and free Coenzyme A, an essential cofactor in various metabolic pathways.

2.6.1. Principle of the Assay

The intracellular ratio of Acyl-CoA to free Coenzyme A (CoASH) was estimated utilizing a coupled enzymatic assay, which converts all CoA forms into a singular detectable product, NADH. The concentration of NADH was subsequently quantified by measuring its absorbance at 340 nm. The assay was performed in two sequential steps.

Total CoA Measurement: Acyl-CoA esters are hydrolyzed by the enzyme acyl-CoA hydrolase, releasing free CoASH. The liberated CoASH, along with the body's endogenous CoASH pools, is then oxidized by α-ketoglutarate dehydrogenase (α-KGDH) in the presence of α-ketoglutarate and NAD^+. This enzymatic process produces NADH in a molar ratio to the total CoA pool, which includes both free CoASH and Acyl-CoA. The following reactions summarize this overall process**.**

(Acyl-CoA + H_2O → CoASH + Fatty Acid) followed by (CoASH + α-Ketoglutarate + NAD^+ → Succinyl-CoA + CO_2 + NADH)

Free CoASH Measurement: In a separate aliquot of the sample, endogenous free CoASH is oxidized by α-KGDH in the absence of acyl-CoA hydrolase, resulting in the production of NADH proportional solely to the free CoASH content. The concentration of acyl-CoA is determined by subtracting the free CoASH value from the total CoA value. Subsequently, the acyl-CoA-to-CoA ratio is calculated from these measurements.

2.6.2. Sample Preparation

After the 72-hour treatment interval, cells cultured in 6-well plates were rinsed with ice-cold PBS and lysed

with 200 µL of 0.6 M perchloric acid. The lysates were then collected, vortexed vigorously, and centrifuged at 15,000 × g for 10 minutes at 4°C to facilitate protein precipitation. The resulting acidic supernatants were neutralized to a pH range of 6-7 by adding 50 µL of 2 M $KHCO_3$, followed by centrifugation to eliminate the precipitated potassium perchlorate salt. The final neutralized extracts were maintained on ice and used immediately for subsequent assays.

2.6.3. Enzymatic Reaction and Spectrophotometric Measurement

All assays were conducted utilizing a 96-well microplate. The reaction mixture for the Total CoA assay comprised 50 mM Tris-HCl (pH 8.0), 2.5 mM α-ketoglutarate, 0.2 mM NAD^+, 2.5 mM $MgCl_2$, 0.1% (v/v) Triton X-100, and 0.2 U/mL of acyl-CoA hydrolase derived from Pseudomonas spp. (Sigma-Aldrich), and 50 µL of neutralized cellular extract. The assay was initiated through the addition of 0.5 U/mL of α-ketoglutarate dehydrogenase (α-KGDH) obtained from porcine heart (Sigma-Aldrich). Variations in absorbance at 340 nm were monitored over 20 minutes at 37°C using a microplate reader. The Free CoASH assay was conducted similarly, excluding the addition of acyl-CoA hydrolase. For each experimental set, a standard curve was generated using known CoASH concentrations ranging from 0 to 10 nmol, thereby enabling conversion of absorbance changes (ΔA_{340}) to nanomoles of CoA.

Using data from six independent biological replicates per treatment group, the concentrations were determined as follows:

Total CoA (nmol) = (ΔA_{340} [Total] × Dilution Factor) / (ε × path length)

Free CoASH (nmol) = (ΔA_{340} [Free] × Dilution Factor) / (ε × path length).

Acyl-CoA (nmol) = Total CoA - Free CoASH.

Acyl-CoA/CoA Ratio = (Acyl-CoA) / (Free CoASH).

Where ε (extinction coefficient for NADH) = 6220 $M^{-1}cm^{-1}$ [39].

2.7. Molecular Docking Assay

The structural configurations of Empagliflozin and Metformin were constructed and optimized using ChemDraw (Cambridge Soft, USA) and Chem3D. Molecular docking simulations were conducted against two crucial metabolic enzymes (Phosphopantetheine Adenylyl transferase (PPAT) and carnitine palmitoyl transferase 1A (CPT1A).

The selection of PPAT and CPT1A as key metabolic targets is justified by their well-established roles in cancer metabolism. Phosphopantetheine Adenylyl transferase (PPAT) is a critical enzyme involved in the biosynthesis of coenzyme A (CoA), which is vital for the proliferation of cancer cells. PPAT catalyzes a rate-limiting step, and its upregulation directly supports increased production of lipids, amino acids, and energy necessary for rapid tumor growth and survival. Concurrently, Carnitine Palmitoyl transferase 1A (CPT1A) functions as the primary enzyme regulating mitochondrial fatty acid oxidation (FAO). This metabolic pathway serves as a key energy source for various cancers, particularly under conditions of metabolic stress, thereby contributing to chemoresistance and inhibiting apoptosis. The frequent overexpression of both PPAT and CPT1A across diverse cancer types highlights their potential as therapeutic targets for disrupting tumor metabolism and impeding cancer progression [40, 41].

The three-dimensional structures of the metabolic enzymes were retrieved from the Protein Data Bank (PDB codes: 8XSK for PPAT and 2LE3 for CPT1A). These structures were utilized in the docking analyses due to their representation of the constitutively active, disease-associated conformations, which are the primary targets for therapeutic inhibition in cancer treatment.

The structures of metabolic enzymes were refined using AutoDock Tools, which helped identify optimal ligand conformations and generate PDBQT files for further analysis. Then, the structures of Empagliflozin, Metformin, and enzymes (PPAT and CPT1A) were imported into AutoDock Tools for docking analysis. The resulting data, including binding energy scores and interaction profiles, were thoroughly examined with BIOVIA Discovery Studio, UCSF Chimera, and AutoDock [42, 43].

2.8. Ethical Approval

Our study only used in vitro cell line models and didn't involve human participants or lab animals. However, we adhered to our institution's ethical guidelines for laboratory research throughout the study.

2.9. Statistical Analysis

Normality of data was assessed using the Shapiro-Wilk test prior to conducting parametric analyses. Cytotoxicity data are expressed as mean ± standard deviation (SD). Differences among experimental

groups were analyzed using one-way analysis of variance (ANOVA). For pairwise comparisons, paired t-tests and LSD post-hoc tests were employed. All statistical procedures were performed with SPSS version 20, with a significance threshold set at $p < 0.05$ [44].

Our study used small and capital letters in data tables to distinguish between statistical groupings and significance levels. When means (averages) have the same letter, it indicates that there is no significant difference. However, when means have different letters, they're statistically significant. We used capital letters to compare means across rows and small letters to compare means across columns. This approach offers a clear and straightforward way to present complex statistical results without lengthy explanations. Readers can easily see which groups are similar or different based on the assigned letters.

3. RESULTS

3.1. Cytotoxic Assay

3.1.1. Cytotoxicity of the (Empagliflozin -Metformin) Mixture

The mixture exhibited significant cytotoxicity against HeLa cells, with effects that intensified over time and at higher concentrations. After 24 hours, cell inhibition ranged from about 1.4% at 0.1 µg/ml to 70% at 1000 µg/ml, while after 72 hours, inhibition increased from approximately 7% to over 81%. The IC_{50} value notably dropped from 504.5 µg/ml at 24 hours to 207.5 µg/ml at 72 hours, indicating greater potency with longer exposure. Conversely, the mixture had minimal effects on human foreskin fibroblasts, highlighting its selectivity for cancer cells. These results suggest that the cytotoxicity of the mixture against HeLa cells is dependent on both concentrations and duration.

Table 1: The Effect of Mixture on the Survival Rates of HeLa and HFF Cell Lines at 24 and 72 Hours

Con. (µg/ml)	Cellular proliferation inhibition (mean ± SD)					
	HeLa cell line			HFF cell line		
	24 hr.	72 hr.	*P*- value	24 hr.	72 hr.	*P*- value
0.1	1.4 ± 0.5 d	7.0 ± 1.2 e	0.012*	0.0 ± 0.0 d	1.0 ± 0.4 d	0.102
1	13.0 ± 1.8 c	22.0 ± 2.1 d	0.003*	2.0 ± 0.7 cd	3.0 ± 0.9 d	0.245
10	18.0 ± 2.0 c	32.0 ± 2.5 c	0.001*	4.0 ± 1.1 c	8.0 ± 1.3 c	0.023*
100	26.0 ± 2.3 b	47.0 ± 3.0 b	0.001*	9.0 ± 1.5 b	13.0 ± 1.8 b	0.041*
1000	70.0 ± 4.1 a	81.0 ± 4.5 a	0.018*	12.0 ± 1.9 a	17.0 ± 2.2 a	0.035*
IC 50	504.5 µg/ml	207.5 µg/ml	-	>1000 µg/ml	>1000 µg/ml	-
LSD value	5.8	6.7	-	2.9	3.5	-

*: indicates $p < 0.05$.

Table 2: Comparing the Mixture's Effects on the Growth of HeLa and HFF Cell Lines at 24 and 72 Hours

Con. (µg/ml)	Cellular proliferation inhibition (mean ± SD)					
	24 hr.			72 hr.		
	HeLa cell line	HFF cell line	*P*- value	HeLa cell line	HFF cell line	*P*- value
0.1	1.4 ± 0.5 d	0.0 ± 0.0 d	0.055	7.0 ± 1.2 e	1.0 ± 0.4 d	0.003*
1	13.0 ± 1.8 c	2.0 ± 0.7 cd	0.001*	22.0 ± 2.1 d	3.0 ± 0.9 d	0.001*
10	18.0 ± 2.0 c	4.0 ± 1.1 c	0.001*	32.0 ± 2.5 c	8.0 ± 1.3 c	0.001*
100	26.0 ± 2.3 b	9.0 ± 1.5 b	0.001*	47.0 ± 3.0 b	13.0 ± 1.8 b	0.001*
1000	70.0 ± 4.1 a	12.0 ± 1.9 a	0.001*	81.0 ± 4.5 a	17.0 ± 2.2 a	0.001*
IC 50	504.5 µg/ml	>1000 µg/ml	-	207.5 µg/ml	>1000 µg/ml	-
LSD value	5.8	2.9	-	6.7	3.5	

*: indicates $p < 0.05$.

Table 3: The Effect of Carboplatin on the Survival Rates of HeLa and HFF Cell Lines at 24 and 72 Hours

Con. (µg/ml)	Cellular proliferation inhibition (mean ± SD)					
	HeLa cell line			HFF cell line		
	24 hr.	72 hr.	*P*- value	24 hr.	72 hr.	*P*- value
0.1	6.0 ± 1.1 e	1.0 ± 0.4 e	0.022*	4.0 ± 1.0 e	10.0 ± 1.6 e	0.019*
1	15.0 ± 1.7 d	5.0 ± 1.0 d	0.007*	17.0 ± 1.9 d	24.0 ± 2.2 d	0.031*
10	25.0 ± 2.2 c	17.0 ± 1.9 c	0.016*	25.0 ± 2.2 c	37.0 ± 2.8 c	0.008*
100	37.0 ± 2.8 b	27.0 ± 2.3 b	0.028*	38.0 ± 2.9 b	53.0 ± 3.2 b	0.006*
1000	57.0 ± 3.3 a	39.0 ± 2.9 a	0.001*	53.0 ± 3.2 a	69.0 ± 3.7 a	0.009*
IC 50	650.2 µg/ml	>1000 µg/ml	-	800.1 µg/ml	81.5 µg/ml	-
LSD value	4.9	3.9	-	4.6	5.5	-

*: significant at (P<0.05).

The outcomes demonstrate that the impact of the mixture on the HFF cell line was lower compared to HeLa cells. After 24 hours, proliferation was minimally affected, with only 12.0 ± 1.9% inhibition at 1000 µg/ml, which increased slightly to 17.0 ± 2.2% after 72 hours. The IC_{50} values exceeded 1000 µg/ml at both time points. Statistical analysis confirmed a significant difference in sensitivity, indicating a selective anti-proliferative effect on cancer cells while sparing normal fibroblasts, as evidenced by the lower inhibition in HFF cells Tables **1**,**2**.

3.1.2. Carboplatin cytotoxicity

The cytotoxic effects of Carboplatin were assessed on HeLa (cervical carcinoma) and HFF (normal human Foreskin Fibroblasts) cell lines over durations of 24 and 72 hours. Results demonstrated a concentration-dependent inhibition of proliferation in both cell types. Notably, HeLa cells exhibited greater sensitivity at the 24-hour mark, with an IC_{50} value of 650.2 µg/ml, which increased markedly by 72 hours (IC_{50} > 1000 µg/ml), suggesting the emergence of resistance. Conversely, HFF cells showed increased susceptibility over time, with IC_{50} values decreasing from 800.1 µg/ml at 24 hours to 81.5 µg/ml at 72 hours. Statistical analysis ($p < 0.05$) confirmed significant differences between time points at each concentration for both cell lines, indicating a time-dependent cytotoxic response. The observed shifts in IC_{50} values imply distinct temporal mechanisms of action in malignant versus normal cells Table **3**.

3.1.3. Cytotoxicity of Mixture Medications Individually

The cytotoxic effects of Empagliflozin and Metformin were systematically examined to understand the mechanisms behind their combined toxicity. Additionally, it investigates the nature of their interactions, determining whether these agents show synergistic, antagonistic, or additive effects.

3.1.3.1. Empagliflozin Cytotoxicity

The antiproliferative effects of Empagliflozin on cervical cancer cells were evaluated at 24 and 72 hours. Results demonstrated a concentration-dependent and time-dependent reduction in cell

Table 4: The Effect of Empagliflozin on the Survival Rates of Cervical Cancer Cells at 24 and 72 Hours

Concentration (µg/ml)	Cellular proliferation inhibition (mean ± SD)		*P*- value
	24 hr.	72 hr.	
0.1	0.0 ± 0.0 d	5.0 ± 1.0 e	0.021*
1	6.0 ± 1.1 c	14.0 ± 1.6 d	0.004*
10	11.0 ± 1.5 b	23.0 ± 2.1 c	0.001*
100	33.0 ± 2.5 a	39.0 ± 2.8 b	0.033*
1000	36.0 ± 2.7 a	51.0 ± 3.1 a	0.001*
IC 50	>1000 µg/ml	916.6 µg/ml	-
LSD value	3.7	4.2	-

*: significant at (P<0.05).

Table 5: The Effect of Metformin on the Survival Rates of Cervical Cancer Cells after 24 and 72 Hours

Concentration (µg/ml)	Cellular proliferation inhibition (mean ± SD)		*P*- value
	24 hr.	72 hr.	
0.1	0.0 ± 0.0 d	5.0 ± 1.0 d	0.018*
1	2.0 ± 0.7 d	21.0 ± 2.0 c	0.001*
10	9.0 ± 1.4 c	28.0 ± 2.3 b	0.001*
100	25.0 ± 2.2 b	32.0 ± 2.5 ab	0.029*
1000	36.0 ± 2.7 a	44.0 ± 2.9 a	0.026*
IC 50	>1000 µg/ml	>1000 µg/ml	-
[b] LSD value	3.5	4.7	-

*: indicates p < 0.05.

viability. After 24 hours, significant inhibition was observed only at higher concentrations, with 100 µg/ml and 1000 µg/ml leading to 33.0% and 36.0% inhibition, respectively. At 72 hours, inhibition was markedly increased, reaching 51.0% at the highest concentration. The IC_{50} decreased from over 1000 µg/ml at 24 hours to 916.6 µg/ml at 72 hours, indicating enhanced potency over time Table **4**.

3.1.3.2. Metformin Cytotoxicity

The study evaluated the effects of metformin on cervical cancer cell growth over 24 and 72 hours. Results showed a concentration- and time-dependent reduction in cell viability, with modest inhibition at 24 hours (up to 36%) and more significant effects after 72 hours (up to 44%). Notably, lower concentrations demonstrated significantly increased inhibition over time, as illustrated by the 1 µg/ml dose, which increased from 2% to 21% inhibition. The IC_{50} exceeded 1000 µg/ml at both time points, indicating that high doses are needed for effectiveness. The statistically significant difference ($p < 0.05$) underscores the importance of prolonged exposure for achieving optimal antiproliferative results Table **5**.

3.1.4. Comparison of Cytotoxicity among Empagliflozin, Metformin, Carboplatin, and the Mixture

The outcomes of the comparison among the various study treatments after 24 and 72 hours revealed the following. Carboplatin demonstrated the most potent inhibitory effect at lower concentrations (1–10 µg/ml), while the combination therapy showed greater efficacy at the highest dose (1000 µg/ml), achieving 70.0 ± 4.1% inhibition. At the 72-hour mark, the combination treatment displayed a significant increase in effectiveness across all concentrations, reaching 81.0 ± 4.5% inhibition at 1000 µg/ml—surpassing the efficacy of all individual agents. The IC_{50} values supported this trend, with the combination exhibiting the lowest IC_{50} at 72 hours (207.5 µg/ml), indicating increased potency over time. Empagliflozin and Metformin produced moderate, dose-dependent responses, but their IC_{50} values remained high (>1000 µg/ml at 24 hours).

Table 6: Comparison of Empagliflozin, Metformin, Carboplatin, and a Combination for Inhibiting the Growth of HeLa Cancer Cells Over 24 Hours

Concentration (µg/ml)	Cellular proliferation inhibition (mean ± SD)				LSD
	Empagliflozin	Metformin	Carboplatin	mix	
0.1	B 0.0 ± 0.0 d	B 0.0 ± 0.0 d	A 6.0 ± 1.1 e	B 1.4 ± 0.5 d	1.7
1	B 6.0 ± 1.1 c	C 2.0 ± 0.7 d	A 15.0 ± 1.7 d	A 13.0 ± 1.8 c	3.6
10	C 11.0 ± 1.5 b	C 9.0 ± 1.4 c	A 25.0 ± 2.2 c	B 18.0 ± 2.0 c	4
100	A 33.0 ± 2.5 a	B 25.0 ± 2.2 b	A 37.0 ± 2.8 b	B 26.0 ± 2.3 b	5.4
1000	C 36.0 ± 2.7 a	C 36.0 ± 2.7 a	B 57.0 ± 3.3 a	A 70.0 ± 4.1 a	7.2
IC 50	>1000 µg/ml	>1000 µg/ml	650.2 µg/ml	504.5 µg/ml	
LSD value	3.7	3.5	4.9	5.8	

*: indicates p < 0.05.

Table 7: Comparison of Empagliflozin, Metformin, Carboplatin, and a Combination for Inhibiting the Growth of HeLa Cancer Cells Over 72 Hours

Concentration (µg/ml)	Cellular proliferation inhibition (mean ± SD)				[b] LSD value
	Empagliflozin	Metformin	Carboplatin	mix	
0.1	A 5.0 ± 1.0 e	A 5.0 ± 1.0 d	B 1.0 ± 0.4 e	A 7.0 ± 1.2 e	2.9
1	B 14.0 ± 1.6 d	A 21.0 ± 2.0 c	C 5.0 ± 1.0 d	A 22.0 ± 2.1 d	3.9
10	B 23.0 ± 2.1 c	A 28.0 ± 2.3 b	C 17.0 ± 1.9 c	A 32.0 ± 2.5 c	4.8
100	B 39.0 ± 2.8 b	C 32.0 ± 2.5 ab	C 27.0 ± 2.3 b	A 47.0 ± 3.0 b	5.7
1000	B 51.0 ± 3.1 a	BC 44.0 ± 2.9 a	C 39.0 ± 2.9 a	A 81.0 ± 4.5 a	7.4
IC 50	916.6 µg/ml	>1000 µg/ml	>1000 µg/ml	207.5 µg/ml	
LSD value	4.2	4.7	3.9	6.7	

*: indicates $p < 0.05$.

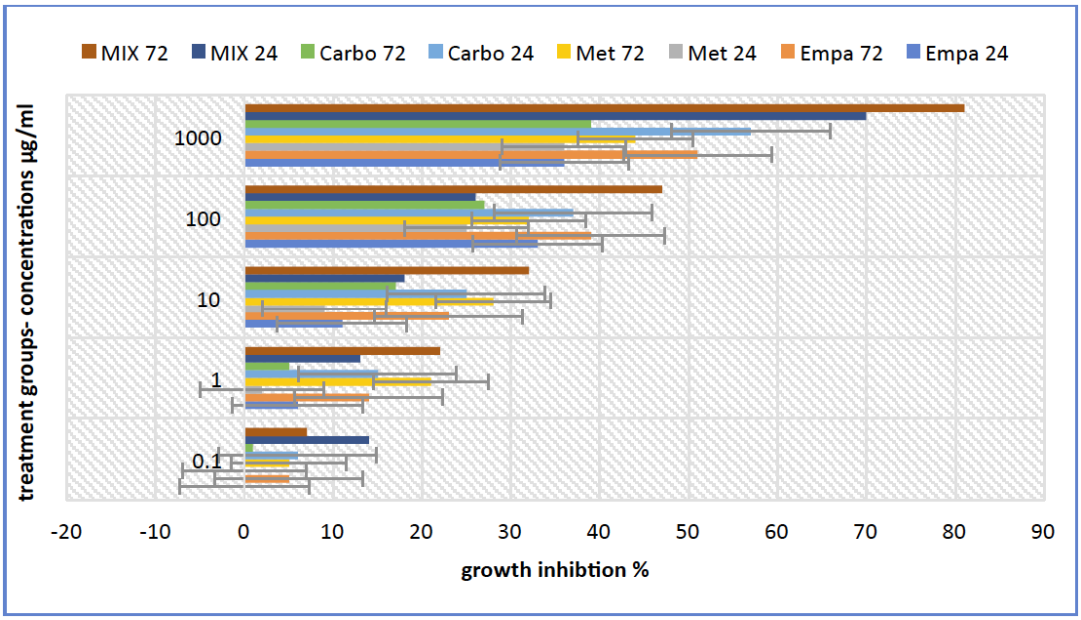

Figure 1: Comparison of Empagliflozin, Metformin, Carboplatin, and Their Combinations in Inhibiting HeLa Cell Growth at 24 and 72 Hours. (**Empa**; Empagliflozin, **Met**; Metformin, **Carbo**; Carboplatin, **MIX**; Empagliflozin – Metformin mixture).

Statistical analysis, including LSD values, identified significant differences between treatments at each concentration ($p < 0.05$), emphasizing the superior and consistent cytotoxic effects of the combination therapy Tables **6**, **7**, Figure **1**.

3.2. Selective Toxicity Assay

The study findings showed that the selectivity index (SI) of the Empagliflozin–Metformin combination increased from 1.98 at 24 hours to 4.82 at 72 hours, indicating greater selectivity for cancer cells over time. In contrast, the SI for carboplatin decreased significantly from 1.23 at 24 hours to 0.08 at 72 hours, suggesting a loss of specificity for targeting cancer cells over time. This decline may reflect the development of resistance mechanisms in cancer cells against carboplatin with prolonged exposure Table **8**.

3.3. Medication Mixture Interaction pattern

3.3.1. Combination Index

After a 24-hour incubation period, the CI score revealed distinct interaction patterns among the mixture components. Specifically, concentrations of 0.1, 1, and 10 µg/ml demonstrated very strong synergistic effects, while the concentrations of 100 and 1000 µg/ml exhibited moderate synergism and a synergistic interaction pattern, respectively.

Following a 72-hour incubation period, the results indicated that concentrations of 1, 10, and 100 µg/ml

Table 8: Selective Toxicity Index (SI) of the Empagliflozin-Metformin Combination and Carboplatin on HeLa vs. HFF Cells

Treatment Group	Incubation Time (hours)	IC_{50} HeLa (Cancer) Cells (µg/ml)	IC_{50} HFF (Normal) Cells (µg/ml)	Selective Index (SI)[a]
Empagliflozin-Metformin Combination	24	504.5	>1000	>1.98
	72	207.5	>1000	>4.82
Carboplatin	24	650.2	800.1	1.23
	72	>1000	81.5	<0.08

[a]: Selective Index (SI) was calculated using the formula: SI = IC_{50} of Normal Cells (HFF) / IC_{50} of Cancer Cells (HeLa). An SI > 1 indicates selectivity towards cancer cells, while an SI < 1 indicates higher toxicity to normal cells.

exhibited strong synergistic effects, whereas the 1000 µg/ml concentration demonstrated a very strong synergistic interaction. Conversely, the 0.1 µg/ml concentration showed a Slight antagonistic effect Tables **9**,**10**, Figure **2**.

3.3.2. Dose Reduction Index

Across all incubation periods and concentrations, the DRI score consistently stayed above 1. This suggests that the combined concentration of each component needed to cause significant cytotoxicity is lower than the individual toxic thresholds seen when compounds are used alone. The lower effective concentrations indicate a decreased risk of adverse effects from the combined formulation, especially compared to the side effects linked with single-agent treatment applications Tables **9**,**10**, Figure **2**.

3.4. Acyl-CoA/CoA Ratio Assessment

The study demonstrated that exposure of HeLa cells to individual agents and their combinations for 72 hours resulted in a statistically significant, dose-

Table 9: CI and DRI for the Combination after a 24-Hour Incubation Period

DRI value		Combination style	CI score	(concentration µg/ml) The ratio of (Empagliflozin- Metformin) in the combination is 1:1		
Metformin	Empagliflozin			Empagliflozin	Metformin	Combination
28.9494*	48.5536*	Very Strong Synergism	0.05514	0.05	0.05	0.1
96.4807*	80.3335*	Very Strong Synergism	0.02281	0.5	0.5	1
85.5566*	63.5349*	Very Strong Synergism	0.02743	5	5	10
3.44840*	2.22637*	Moderate Synergism	0.73915	50	50	100
5.78839*	2.12764*	Synergism	0.64276	500	500	1000

Compusyn software was used to determine the values of the Combination Index (CI) and Dose Reduction Index (DRI). A CI value greater than 1 indicates antagonism, a CI equal to 1 signifies an additive effect, and a CI less than 1 suggests synergism. A DRI value over 1 indicates reduced toxicity. An asterisk (*) signifies a beneficial decrease in the effective cytotoxic concentration [45].

Table 10: CI and DRI for the Combination after a 72-Hour Incubation Period

DRI value		Combination style	CI score	(concentration µg/ml) The ratio of (Empagliflozin- Metformin) in the combination is 1:1		
Metformin	Empagliflozin			Empagliflozin	Metformin	Combination
1.12489*	3.26076*	Slight Antagonism	1.19566	0.05	0.05	0.1
18.2400*	20.5990*	Strong Synergism	0.10337	0.5	0.5	1
13.1028*	10.2695*	Strong Synergism	0.17370	5	5	10
15.0434*	7.50187*	Strong Synergism	0.19977	50	50	100
636.841*	103.576*	Very Strong Synergism	0.01123	500	500	1000

Compusyn software was used to determine the values of the Combination Index (CI) and Dose Reduction Index (DRI). A CI value greater than 1 indicates antagonism, a CI equal to 1 signifies an additive effect, and a CI less than 1 suggests synergism. A DRI value over 1 indicates reduced toxicity. An asterisk (*) signifies a beneficial decrease in the effective cytotoxic concentration [45].

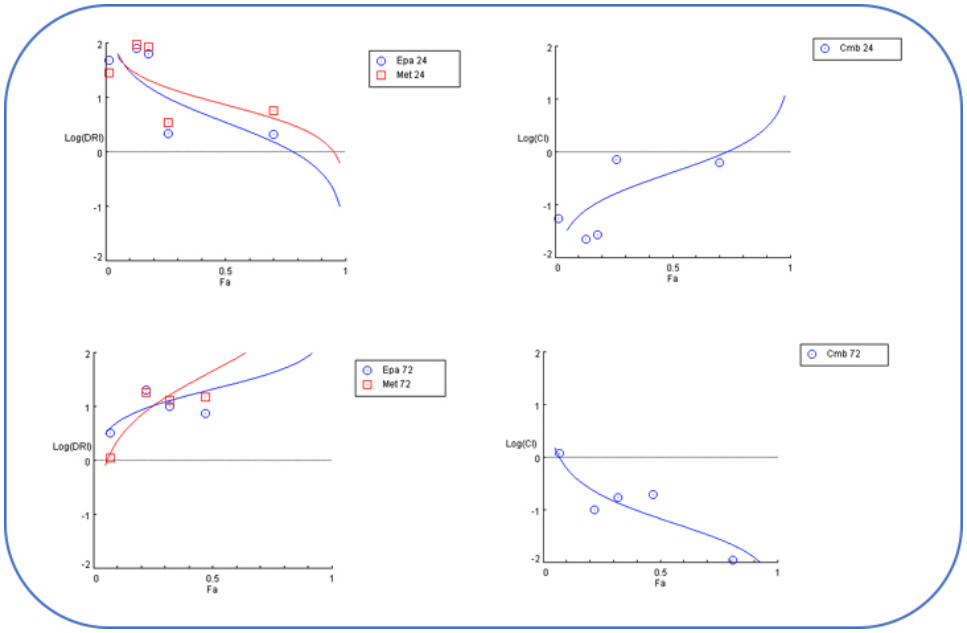

Figure 2: Plots show the combination index (CI) on the left and the dose reduction index (DRI) on the right for the mixture after 24 hours (above) and 72 hours (below) of incubation. **Epa**: Empagliflozin, **Met**: Metformin, **CI**: combination index, **DRI**: dose reduction index.

dependent elevation in the Acyl-CoA/CoA ratio relative to the untreated control (baseline, 1.0 ± 0.09). Specifically, treatment with empagliflozin at a concentration of 1000 µg/ml yielded a moderate increase, elevating the ratio to 1.92 ± 0.14. Metformin at the same concentration induced a more pronounced effect, raising the ratio to 2.58 ± 0.19. Additionally, the chemotherapeutic agent carboplatin, administered at 1000 µg/ml, increased the ratio to 2.25 ± 0.18.

Strikingly, the combination of Empagliflozin and Metformin caused a significantly greater disruption in CoA pool homeostasis. At the highest concentration tested (1000 µg/ml, with each drug at 500 µg/ml), this combination produced an Acyl-CoA/CoA ratio of 5.02 ± 0.41. This ratio was not only significantly higher than the control group ($p < 0.001$), but also significantly exceeded the effects seen with either drug alone at the same concentrations ($p < 0.001$ for Empagliflozin; $p < 0.01$ for Metformin).

Furthermore, it was more than twice the ratio caused by Carboplatin treatment ($p < 0.001$). Notably, even at a lower concentration (100 µg/ml, with each drug at 50 µg/ml), the combination resulted in a ratio of 3.28 ± 0.27, indicating a synergistic metabolic disruption Table **11**.

3.5. Molecular Docking Studies

Molecular docking simulations were used to explore the interaction of Empagliflozin and Metformin with key metabolic enzymes. The study focused on Phosphopantetheine Adenylyltransferase (PPAT, PDB code: 8XSK) and Carnitine Palmitoyltransferase 1A (CPT1A, PDB code: 2LE3). These enzymes were chosen because they represent stable, disease-related structures that serve as potential targets for cancer therapy. Tools used in this research included AutoDock Tools version 1.5.7, BIOVIA Discovery Studio, UCSF Chimera, and AutoDock Vina [46].

3.5.1. Docking with Phosphopantetheine Adenylyl Transferase Enzyme

The chemical docking study showed that Empagliflozin interacts with the PPAT metabolic enzyme, with a docking score of -7.4 kcal/mol. Molecular docking analysis identified one "hydrogen electrostatics bond" with amino acid residues of HIS A:18 at a distance of 3.14 Å. Additionally, a two-electrostatics bond occurs with LYS A:42 at 3.28 Å. and ARG A:133 at 3.97 Å. And finally, a two-hydrophobic bond occurs with LYS A:42 at 4.23 Å. and 5.48 Å—Figure **3**.

The other component in the mixture, Metformin, exhibited the capacity to interact with the PPAT metabolic enzyme, as evidenced by a docking score of -5.2 kcal/mol. Molecular docking analysis revealed the formation of three conventional hydrogen bonds with the amino acid residues ARG A:91, GLU A:99, and TYR A:7, at distances of 2.65 Å, 2.90 Å, and 1.94 Å, respectively Figure **3**.

Table 11: Effect of Empagliflozin, Metformin, Carboplatin, and (Empagliflozin, Metformin) Combination on the Acyl-CoA/CoA Ratio in HeLa Cells after 72 Hours of Treatment

Treatment	Concentration (µg/ml)	Acyl-CoA/CoA Ratio (Mean ± SD)	Statistical Significance vs. Control	Statistical Significance vs. Combination (1000 µg/ml)
Control	-	1.00 ± 0.09 g	-	p < 0.001
Empagliflozin	100	1.38 ± 0.10 fg	N. S	p < 0.001
	1000	1.92 ± 0.14 de	p < 0.001	p < 0.001
Metformin	100	1.97 ± 0.16 de	p < 0.001	p < 0.001
	1000	2.58 ± 0.19 c	p < 0.001	p < 0.01
Carboplatin	100	1.71 ± 0.13 ef	p < 0.001	p < 0.001
	1000	2.25 ± 0.18 cd	p < 0.001	p < 0.001
Combination (Empa+Met)	100 (50+50)	3.28 ± 0.27 b	p < 0.001	p < 0.01
	1000 (500+500)	5.02 ± 0.41 a	p < 0.001	-
[b] **LSD value**	-	0.42	-	

Values are reported as the mean ± standard deviation (SD) based on six independent replicates (n=6). The untreated control ratio is normalized to a baseline of 1.0. Different superscript letters (a–g) indicate statistically significant differences between all treatment groups ($p < 0.05$), as determined by one-way ANOVA followed by LSD post-hoc analysis. Means sharing the same letter are not significantly different.

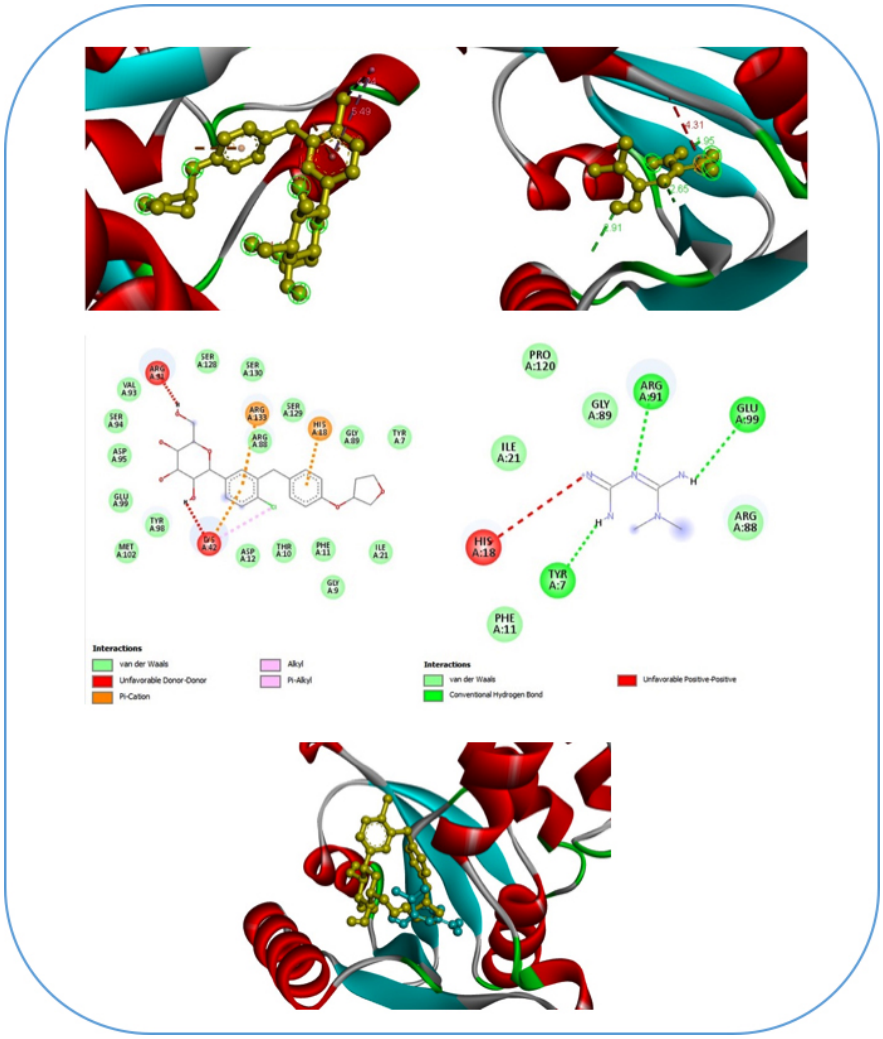

Figure 3: The structural configurations of PPAT binding sites are depicted in both two-dimensional (middle image) and three-dimensional (top image) representations. Empagliflozin and Metformin are presented sequentially from left to right. The lower three-dimensional view highlights the binding sites of the mixture (Empagliflozin (yellow) and Metformin (bright yellow)) on PPAT.

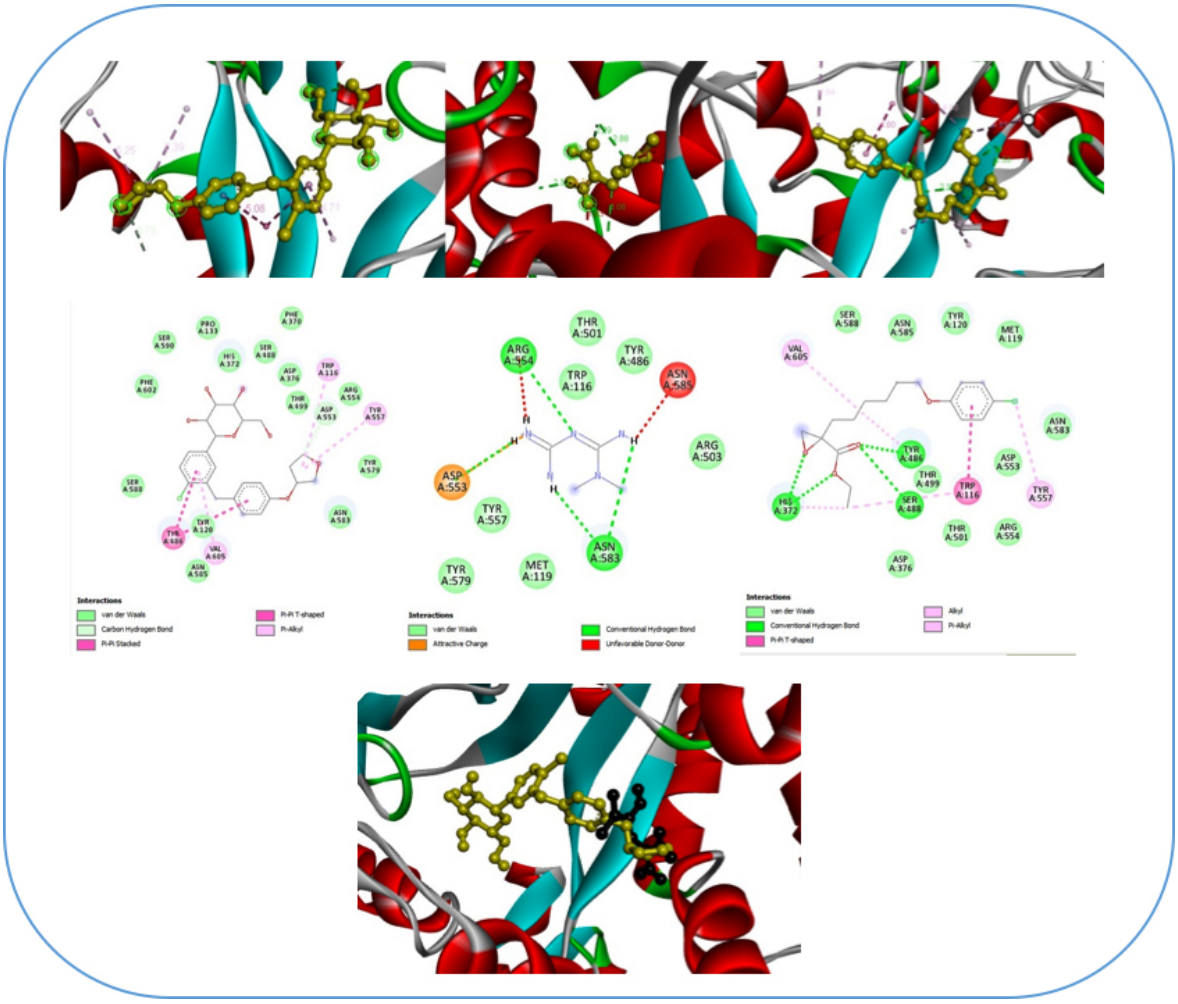

Figure 4: The structural arrangements of CPT1A binding sites are shown in both 2D and 3D views (middle and top images, respectively). Empagliflozin, Metformin, and Etomoxir are displayed from left to right. The lower 3D image shows the binding sites of the mixture (Empagliflozin (yellow) and Metformin (black)) to PDK1.

3.5.2. Docking with Carnitine Palmitoyl Transferase Enzyme

The molecular docking analysis of the interaction between Carnitine Palmitoyl Transferase 1A (CPT1A) and Empagliflozin revealed a docking score of -8.7 kcal/mol. The study identified a single carbon-hydrogen bond with the amino acid residue ASP A:553 at a distance of 3.79 Å. Additionally, a pi-pi stacked interaction was observed with TYR A:486 at 4.45 Å, along with a pi-pi T-shaped interaction involving the same residue at 5.86 Å. An unconventional hydrogen bond was detected with an unidentified amino acid at 2.39 Å. Furthermore, three pi-alkyl interactions were identified with TRP A:116, TYR A:557, and VAL A:605 at distances of 5.38 Å, 5.24 Å, and 4.70 Å, respectively Refer to Figure **4**.

Moreover, the interaction between Metformin and the CPT1A metabolic enzyme was evaluated through molecular docking analysis, which yielded a docking score of -5.1 kcal/mol. The analysis revealed the formation of four conventional hydrogen bonds with amino acid residues ARG A:554, ASN A:583, ASP A:553, and ASN A:583, at distances of 3.07 Å, 2.88 Å, 2.31 Å, and 2.28 Å, respectively. Additionally, an electrostatic interaction was observed with the ASP A:553 residue at a distance of 4.74 Å Figure **4**.

For comparison, a molecular docking study evaluated the interaction between Etomoxir (a CPT1A inhibitor) [47] And a CPT1A metabolic enzyme, resulting in a docking score of -6.4 kcal/mol for binding. The study identified four conventional hydrogen bonds involving the following amino acid residues: HIS A:372 (observed twice), TYR A:486, and SER A:488. The respective bond distances were 2.53 Å, 2.19 Å, 2.38 Å, and 3.05 Å. Additionally, a pi-pi T-shaped interaction was identified with TRP A:116 at a distance of 4.47 Å. An alkyl interaction was also observed with VAL A:605 at 4.67 Å. Furthermore, four pi-alkyl interactions were detected involving TRP A:116, HIS A:372, TYR A:486,

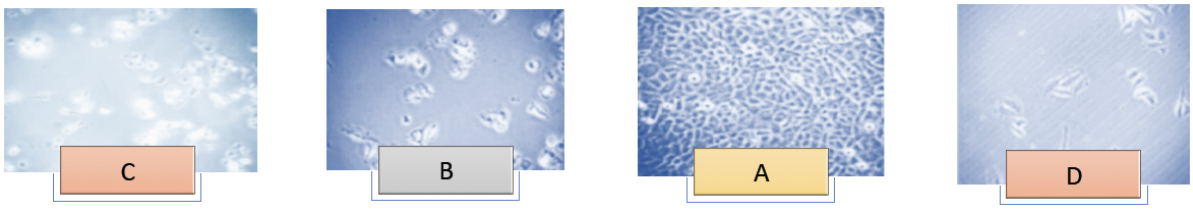

Figure 5: Morphological features of HeLa cells were observed using an inverted microscope at 400× magnification. (**A**) Untreated HeLa cells. (**B**) HeLa cells were treated with 100 µg/mL of Empagliflozin for 72 hours. (**C**) HeLa cells were exposed to 1,000 µg/mL of Metformin for 72 hours. (**D**) HeLa cells were treated with a 1,000 µg/mL mixture for 72 hours.

Table 12: Compares the Molecular Docking Scores of each Component within the Mixtures to those of a Standard Medication Targeting the PPAT and CPT1A Metabolic Enzymes

Receptor	Ligands		
	Empagliflozin	Metformin	Etomoxir
PPAT	-7.4	-5.2	-
CPT1A	-8.7	-5.1	10.4

PPAT: Phosphopantetheine Adenylyl Transferase enzyme. **CPT1A**: Carnitine Palmitoyl Transferase enzyme. Docking scores (in kcal/mol) show predicted binding affinity, with more negative values indicating stronger binding. The scores for standard inhibitors (Etomoxir for CPT1A, while for PPAT, there is no identified direct inhibitor). These are provided for comparison and were calculated using the same molecular docking method and metabolic enzyme (PDB: 8XSK for PPAT and 2LE3 for CPT1A) as the test compounds. A dash (—) indicates that the docking simulation was not performed for that specific drug-target pair.

and TYR A:557, with distances of 4.67 Å, 4.80 Å, 3.76 Å, and 4.63 Å, respectively Figure **5**.

Given the interactions of each mixture component with PPAT and CPT1A, it is proposed that the combined mechanism operates via complementary pathways. This is attributed to the fact that each medication binds to a specific site on the enzymes, thereby producing a synergistic effect among the components Figure **4**.

To elucidate the efficacy of the mixture against PPAT and CPT1A metabolic enzymes, the docking scores of its constituents were compared with those of standard drugs targeting the same enzymes (Table **12**).

3.6. Histopathological Features of the Study Cell Lines

Figure **5** illustrates the morphological alterations observed in the HeLa cell line following a 72-hour treatment period.

4. DISCUSSION

The management of advanced cervical cancer encounters significant challenges due to chemoresistance and the substantial toxicities associated with conventional therapies. This study explores the potential of repurposing Empagliflozin and Metformin as a novel combinatorial therapeutic strategy. To assess this approach, various assays were employed: the MTT assay for quantifying cytotoxic effects, the Selective Index (SI) for evaluating cancer cell specificity, and the Combination Index (CI) in conjunction with the Dose Reduction Index (DRI) to analyze drug interactions. Additionally, the Acyl-CoA/CoA ratio was measured to investigate metabolic disruption, and molecular docking studies were conducted to predict interactions with key metabolic enzymes.

The study findings demonstrate that the combination of Empagliflozin and Metformin exhibits significant, time-dependent cytotoxicity against HeLa cells, characterized by a markedly lower IC_{50} compared to each agent when used individually. Notably, the elevated SI values support the compound's selectivity for malignant cells over normal healthy cells. The combination index (CI) analysis reveals strong synergism. In contrast, favorable drug response index (DRI) scores suggest the potential for concentration reduction, leading to fewer mixture adverse effects compared to using each medication alone. Mechanistically, this combination induces a notable, dose-dependent increase in the Acyl-CoA/CoA ratio, indicating substantial metabolic stress. This is further supported by in silico docking studies, which demonstrate the binding affinity of both drugs to key metabolic regulators PPAT and CPT1A. Collectively, these results suggest that the Empagliflozin-Metformin combination synergistically impairs critical metabolic pathways in cervical cancer cells.

The anticancer mechanisms of the combined empagliflozin and metformin can be explained through two main pathways. The first pathway is based on previous research showing the individual anticancer effects of empagliflozin and metformin. The second involves findings from our study assays, as measured by the Acyl-CoA/CoA ratio, along with in silico molecular docking analyses.

Our results revealed that empagliflozin exhibits a definitive, concentration- and time-dependent cytotoxic effect in HeLa cells, with the IC_{50} value decreasing from over 1000 µg/mL at 24 hours to 916.6 µg/mL at 72 hours. This finding aligns with an expanding body of literature on the antineoplastic properties of SGLT2 inhibitors. For instance, a previous study has demonstrated that canagliflozin induces apoptosis and endoplasmic reticulum stress in HepG2 cells, suggesting a potential class effect extending beyond glycemic regulation [14]. Similarly, a separate study indicated that these agents can inhibit proliferation across various cancer models by disrupting cellular energy metabolism [48-52]. The moderate effectiveness observed with individual agents supports the notion that SGLT2 inhibitors are most effective when used as sensitizing agents. This is confirmed by the strong synergistic effect seen with metformin, a well-documented drug that affects AMPK activity and mitochondrial function [16, 48].

This study demonstrates that metformin exhibits a concentration- and time-dependent antiproliferative effect on HeLa cells. Specifically, inhibition rates increased from 36% at 24 hours to 44% at 72 hours at a concentration of 1000 µg/mL. These findings align with the existing literature on metformin's anticancer properties, which are primarily attributed to its activation of AMP-activated protein kinase (AMPK) and inhibition of mitochondrial complex I, resulting in disrupted cellular energy production. For instance, research has indicated that metformin exerts selective cytotoxicity against breast cancer cell lines, with enhanced efficacy observed at 72 hours, corroborating the time-dependent effects reported herein [18]. Furthermore, an additional study has investigated the application of metformin within innovative drug delivery systems for cervical cancer, thereby underscoring its potential as a candidate for drug repurposing [19, 53].

The moderate activity of a single agent observed in our study is consistent with existing literature, suggesting that its principal efficacy may be realized through combination therapies. The notable synergistic effect observed with empagliflozin underscores this point, emphasizing the importance of incorporating metformin into multi-targeted metabolic strategies for cancer therapy.

Furthermore, building upon the previously described mechanism of anticancer activity for each drug, this study emphasizes the exploration of a novel mechanism involving the modulation of the Acyl-CoA/CoA ratio. The observed concentration-dependent increase in the Acyl-CoA to CoA ratio resulting from the combination of Empagliflozin and Metformin underscores a critical mechanism in anticancer activity rooted in metabolic disruption. This combination (mean ratio: 5.02 ± 0.41) exhibits a significantly greater effect compared to each agent administered independently, indicating a substantial disturbance in the CoA pool equilibrium.

The accumulation of acyl-CoA esters alongside a decrease in free CoASH directly compromises mitochondrial function by inhibiting essential enzymes, including α-ketoglutarate dehydrogenase. Such inhibition impairs the tricarboxylic acid (TCA) cycle and subsequently reduces ATP synthesis, elucidating a potential metabolic target for therapeutic intervention [54]. Such a pronounced metabolic lesion has a particularly detrimental impact on cancer cells, which rely heavily on enhanced CoA metabolism to meet their anabolic requirements and promote cellular proliferation [22]. This targeted induction of metabolic catastrophe is the main mechanism responsible for the mixture's ability to kill cervical cancer cells.

Along with the previously identified underlying anticancer mechanism of the mixture, a molecular docking study was conducted to further support this mechanism by analyzing the ability of the mixture's drugs to target two key metabolic enzymes: Phosphopantetheine Adenylyltransferase (PPAT) and Carnitine Palmitoyltransferase 1A (CPT1A) [55].

The selection of these metabolic enzymes for molecular docking was informed by their pivotal roles in CoA and fatty acid metabolic pathways, thereby establishing a mechanistic link to the anticancer effects observed with the mixture through its modulation of the Acyl-CoA/CoA ratio. Specifically, PPAT catalyzes a rate-limiting step in CoA biosynthesis, which is critical for cancer cell proliferation. Concurrently, CPT1A regulates the rate-limiting step of mitochondrial fatty acid oxidation (FAO), a crucial metabolic pathway activated under conditions of cellular metabolic stress [27, 28]. The significant disruption of the Acyl-CoA/CoA

balance caused by the drug combination indicates a targeted assault on these metabolic points, reducing free CoASH levels and building up lipid intermediates to induce metabolic failure [40, 41].

The molecular docking findings provide a structural basis for elucidating the anticancer mechanism of the compound mixture, illustrating the binding modalities of each drug in relation to their physicochemical properties. Empagliflozin, characterized by a substantial and lipophilic scaffold, demonstrated superior binding energies (PPAT: -7.4 kcal/mol; CPT1A: -8.7 kcal/mol), which facilitate its insertion into hydrophobic pockets within the target sites. This behavior aligns with the binding patterns observed in other rigid, polycyclic molecular frameworks interacting with enzyme active sites [56]. In contrast, the small, polar diguanide structure of Metformin facilitates strong and specific hydrogen bonding interactions with residues in the active site. This interaction pattern is characteristic of highly polar ligands that target metabolic enzymes [57].

Notably, the two compounds bind to distinct amino acid residues on both PPAT and CPT1A. This structural complementarity suggests a mechanism of simultaneous, non-competitive inhibition —a strategy recognized to enhance therapeutic efficacy and circumvent compensatory pathways in cancer treatment [49]. By simultaneously targeting CoA biosynthesis through PPAT inhibition and mitochondrial fatty acid uptake via CPT1A inhibition at different sites, the combination significantly disrupts cellular energy metabolism. This mechanism explains the severe metabolic stress indicated by the increased Acyl-CoA/CoA ratio.

The study's findings indicate a pronounced synergistic interaction between empagliflozin and metformin. This is evidenced by Combination Index (CI) values substantially below one and favorable Dose Reduction Index (DRI) scores, reflecting an enhanced cooperative cytotoxic effect against HeLa cells. The underlying mechanism appears to involve substantial disruption of metabolic homeostasis. Notably, the combination therapy elicited a significant, synergistic increase in the Acyl-CoA/CoA ratio, far exceeding the effects observed with either agent alone, thereby indicating severe impairment of mitochondrial function and energy metabolism. Molecular docking analyses provide structural insights into this synergy, revealing that empagliflozin and metformin bind to distinct sites on the metabolic enzymes PPAT and CPT1A. This dual-binding modality suggests a complementary inhibition strategy targeting CoA biosynthesis and fatty acid oxidation, which collectively precipitate metabolic catastrophe and induce cell death.

Despite the well-established pharmacokinetics and safety profiles of empagliflozin and metformin individually, a key limitation of this study is its exclusive in vitro nature. This model cannot replicate the complex systemic interactions and tumor microenvironment of a living organism. Therefore, future in vivo studies are essential to confirm the therapeutic efficacy and safety of this repurposed combination before clinical translation.

5. CONCLUSION

Managing advanced cervical cancer continues to pose a significant clinical challenge, primarily due to the limitations associated with conventional chemotherapeutic regimens. These include the emergence of chemoresistance and the occurrence of severe toxic side effects, which restrict dosage administration. To mitigate these issues, this study investigates a novel drug repurposing strategy that combines the use of the anti-diabetic agents empagliflozin and metformin.

The objective of this investigation was to assess the potential synergistic cytotoxic and selective effects of the combination treatment on HeLa cervical cancer cells compared with normal human fibroblasts. A comprehensive methodological framework was employed, including MTT assays for cytotoxicity, calculation of selectivity and combination index, evaluation of metabolic disruption via the Acyl-CoA/CoA ratio, and in silico molecular docking analyses targeting the key metabolic enzymes PPAT and CPT1A.

The findings demonstrated that the combination of empagliflozin and metformin exerts potent, temporally dependent cytotoxic effects on neoplastic cells, with an IC50 significantly lower than that of either agent administered independently. Furthermore, the combination exhibited high selectivity for malignant cells relative to normal counterparts. Analytical assessments revealed a robust synergistic interaction, accompanied by a favorable dose reduction index. Mechanistically, this therapeutic synergy appears to induce substantial disruptions in cellular metabolism, as evidenced by a synergistic elevation in the Acyl-CoA/CoA ratio. Molecular docking studies further suggested that these effects may stem from the agents'

complementary binding to and inhibition of key metabolic enzymes PPAT and CPT1A.

The findings of this study provide compelling preclinical evidence supporting the potential repurposing of empagliflozin and metformin as a targeted and synergistic therapeutic approach for cervical cancer. This strategy seems to induce metabolic catastrophe, warranting further exploration through in vivo and clinical investigations.

AUTHOR CONTRIBUTIONS

Design and Development

Ali Muafaq Said, Ayat Ali Salih, Mohammed Abdulridha Obid.

Gathering and Organizing Data

Ali Muafaq Said, Azal Hamoody Jumaa.

Data Analysis/Interpretation

Ayat Ali Salih, Youssef Shakuri

Article Composition

Mohammed Abdulridha Obid, Azal Hamoody Jumaa.

Critique the Essay for Significant Idea

Ali Muafaq Said, Ayat Ali Salih.

Statistical Analysis Expertise

Ayat Ali Salih, Mohammed Abdulridha Obid.

Ultimate Article Endorsement and Guarantee

Mohammed Abdulridha Obid.

ACKNOWLEDGEMENTS

The research team sincerely expresses their heartfelt gratitude to the researchers and instructional staff at ICMGR/Al-Mustansiriyah University and the Iraqi National Cancer Research Centre/University of Baghdad for their invaluable support during this study. We are also deeply grateful to the quality control team at Samarra Pharmaceutical Factory for providing the drugs used in this research.

FINANCIAL SUPPORT AND SPONSORSHIP

Self-funded.

CONFLICTS OF INTEREST

The authors state that they have no conflicts of interest.

ABBREVIATIONS

ICCMGR = The Iraqi Centre for Cancer and Medical Genetics Research.

MTT = 3-(4,5-dimethylthiazol-2-yl)-2,5-diphenyltetrazolium bromide stain

MEM = Minimum Essential Medium

SAS = Statistical Analysis System

SD = Standard deviation

LSD = Least Significant Difference

DRI = dose reduction index

CI = combination index

HFF cell line = human-derived Foreskin Fibroblast cell line

PDB = Protein Data Bank

SGLT2 = sodium-glucose cotransporter 2

PPAT = Phosphopantetheine Adenylyl transferase

CPT1A = carnitine palmitoyl transferase 1A

CoA = Coenzyme A

Acyl-CoA = acylated Coenzyme A

CoASH = free Coenzyme A

REFERENCES

[1] Sung H, Ferlay J, Siegel RL, Laversanne M, Soerjomataram I, Jemal A, *et al*. Global cancer statistics 2020: Globocan estimates of incidence and mortality worldwide for 36 cancers in 185 countries. CA: A Cancer Journal for Clinicians 2021; 71(3): 209-49. https://doi.org/10.3322/caac.21660

[2] Singh D, Vignat J, Lorenzoni V, Eslahi M, Ginsburg O, Lauby-Secretan B, *et al*. Global estimates of incidence and mortality of cervical cancer in 2020: a baseline analysis of the WHO Global Cervical Cancer Elimination Initiative. The Lancet Global Health 2023; 11(2): e197-e206. https://doi.org/10.1016/S2214-109X(22)00501-0

[3] Shahzad A, ur Rehman A, Naz T, Rasool MF, Saeed A, Rasheed S, *et al*. Addition of Bevacizumab to Chemotherapy and Its Impact on Clinical Efficacy in Cervical Cancer: A Systematic Review and Meta-Analysis. Pharmacy 2024; 12(6): 180. https://doi.org/10.3390/pharmacy12060180

[4] Pangarkar K. Development of cisplatin as an anti-cancer Drug 2025.

[5] Masuda T, Tsuruda Y, Matsumoto Y, Uchida H, Nakayama KI, Mimori K. Drug repositioning in cancer: The current situation in Japan. Cancer Science 2020; 111(4): 1039-46. https://doi.org/10.1111/cas.14318

[6] Wieder R, Adam N. Drug repositioning for cancer in the era of AI, big omics, and real-world data. Critical Reviews in Oncology/Hematology 2022; 175: 103730. https://doi.org/10.1016/j.critrevonc.2022.103730

[7] Yousif BJ, Abd Alwahab DH, Mohammed HA, Yasin YS, Jumaa AH. Antiproliferative Potential of Linagliptin-Rivaroxaban Mixture in Cervical Cancer: Mechanistic Insights into Targeting Mutant MAPK, RAS kinase Signal Protein. Asian Pacific Journal of Cancer Prevention 2025; 26(8): 3053-64. https://doi.org/10.31557/APJCP.2025.26.8.3053

[8] Salih SR, Abdulla KN, K Awn A, Yasin YS, Jumaa AH. Impact of Esomeprazole, Ciprofloxacin and Their Combination on Cervical Cancer Cell Line Proliferation: A Focus on Heat Shock Protein 70 Modulation. Asian Pacific Journal of Cancer Prevention 2025; 26(7): 2455-66. https://doi.org/10.31557/APJCP.2025.26.7.2455

[9] Al-Mahdwi TT, Said AM, Hade IM, Yasin YS, Jumaa AH. Synergistic Cytotoxic Impact of Linagliptin-Ciprofloxacin Combination on Cervical Cancer Cell Line: Insights into Targeting Heat Shock Protein 60. Asian Pacific Journal of Cancer Prevention: APJCP 2025; 26(6): 2117. https://doi.org/10.31557/APJCP.2025.26.6.2117

[10] Abdulla KN, Khudhur RK, Said AM, Jumaa AH, Yasin YS. Laetrile and Methotrexate: A Dual-Drug Approach to Inhibiting Cervical Cancer Cell Proliferation. Journal of Cancer Research Updates 2025; 14: 52-62. https://doi.org/10.30683/1929-2279.2025.14.06

[11] Ahmed A, Nihad A, Sabreen G, Yasin YS, Azal J. Synergistic Antiproliferative Effect of Linagliptin-Metformin Combination on the Growth of Hela Cancer Cell Line. Journal of Cancer Research Updates 2025; 14: 12-23. https://doi.org/10.30683/1929-2279.2025.14.02

[12] Jumaa AH, Hade IM, Abdulla KN, Yasin YS. Ciprofloxacin and Metformin as Dual Therapeutic Agents: Synergistic Impact on Cervical Cancer Cell line Proliferation: Insight into Cytoplasmic SRC Tyrosine Kinase Targeting. Asian Pacific Journal of Cancer Biology 2025; 10(3): 699-712. https://doi.org/10.31557/apjcb.2025.10.3.699-712

[13] Khudhur RK, Yahiya YI, Majeed AH, Yasin YS, Jumaa AH. Scrutiny of the Co-Cytotoxic Impact of Metformin-Omeprazole on the Cervical Cancer Cell Line and Their Aptitude to Target Heat Shock 60. Asian Pacific Journal of Cancer Prevention: APJCP 2025; 26(4): 1353. https://doi.org/10.31557/APJCP.2025.26.4.1353

[14] Abdel-Rafei MK, Thabet NM, Rashed LA, Moustafa EM. Canagliflozin, a SGLT-2 inhibitor, relieves ER stress, modulates autophagy and induces apoptosis in irradiated HepG2 cells: signal transduction between PI3K/AKT/GSK-3β/mTOR and Wnt/β-catenin pathways; *in vitro*. Journal of Cancer Research and Therapeutics 2021; 17(6): 1404-18. https://doi.org/10.4103/jcrt.JCRT_963_19

[15] Dong W, Wang Y, Fan S. Potential anticancer effects of sodium-glucose cotransporter protein 2 (SGLT2) inhibitors Canagliflozin and Dapagliflozin. Cancer Chemotherapy and Pharmacology 2025; 95(1): 63. https://doi.org/10.1007/s00280-025-04788-3

[16] Buczyńska A, Sidorkiewicz I, Krętowski AJ, Zbucka-Krętowska M, Adamska A. Metformin intervention—A panacea for cancer treatment? Cancers 2022; 14(5): 1336. https://doi.org/10.3390/cancers14051336

[17] Buczyńska A, Sidorkiewicz I, Krętowski A, Zbucka-Krętowska M, Adamska A. Metformin Intervention—A Panacea for Cancer Treatment? Cancers 2022, 14, 1336. s Note: MDPI stays neutral with regard to jurisdictional claims in published 2022. https://doi.org/10.3390/cancers14051336

[18] Islam SR, Manna SK. Identification of glucose-independent and reversible metabolic pathways associated with anti-proliferative effect of metformin in liver cancer cells. Metabolomics 2024; 20(2): 29. https://doi.org/10.1007/s11306-024-02096-0

[19] Van Nostrand JL, Hellberg K, Luo E-C, Van Nostrand EL, Dayn A, Yu J, *et al*. AMPK regulation of Raptor and TSC2 mediate metformin effects on transcriptional control of anabolism and inflammation. Genes & Development 2020; 34(19-20): 1330-44. https://doi.org/10.1101/gad.339895.120

[20] Hanahan D. Hallmarks of cancer: new dimensions. Cancer Discovery 2022; 12(1): 31-46. https://doi.org/10.1158/2159-8290.CD-21-1059

[21] Trefely S, Lovell CD, Snyder NW, Wellen KE. Compartmentalised acyl-CoA metabolism and roles in chromatin regulation. Molecular Metabolism 2020; 38: 100941. https://doi.org/10.1016/j.molmet.2020.01.005

[22] Guertin DA, Wellen KE. Acetyl-CoA metabolism in cancer. Nature Reviews Cancer 2023; 23(3): 156-72. https://doi.org/10.1038/s41568-022-00543-5

[23] Pougovkina O, Te Brinke H, Wanders RJ, Houten SM, de Boer VC. Aberrant protein acylation is a common observation in inborn errors of acyl-CoA metabolism. Journal of Inherited Metabolic Disease 2014; 37(5): 709-14. https://doi.org/10.1007/s10545-014-9684-9

[24] Leonardi R, Zhang Y-M, Rock CO, Jackowski S. Coenzyme A: back in action. Progress in Lipid Research 2005; 44(2-3): 125-53. https://doi.org/10.1016/j.plipres.2005.04.001

[25] Qu Q, Zeng F, Liu X, Wang Q, Deng F. Fatty acid oxidation and carnitine palmitoyltransferase I: emerging therapeutic targets in cancer. Cell Death & Disease 2016; 7(5): e2226-e. https://doi.org/10.1038/cddis.2016.132

[26] Arean AG, Jumaa AH, Hashim WS, Mohamed AA, Yasin YS. The cytotoxic effect of ephedra transitoria on hela cancer cell line: bio-engineering.

[27] Liu B, Song M, Qin H, Zhang B, Liu Y, Sun Y, *et al*. Phosphoribosyl pyrophosphate amidotransferase promotes the progression of thyroid cancer via regulating pyruvate kinase M2. OncoTargets and Therapy 2020: 7629-39. https://doi.org/10.2147/OTT.S253137

[28] Ma L, Chen C, Zhao C, Li T, Ma L, Jiang J, *et al*. Targeting carnitine palmitoyl transferase 1A (CPT1A) induces ferroptosis and synergizes with immunotherapy in lung cancer. Signal Transduction and Targeted Therapy 2024; 9(1): 64. https://doi.org/10.1038/s41392-024-01772-w

[29] Saboowala HK. What HeLa Cells aka Immortal Cells Are and Why They Are Important. An Example of Racism in Medicine: Dr. Hakim Saboowala; 2022.

[30] Lyapun I, Andryukov B, Bynina M. HeLa cell culture: Immortal heritage of henrietta lacks. Molecular Genetics, Microbiology and Virology 2019; 34(4): 195-200. https://doi.org/10.3103/S0891416819040050

[31] Nadalutti CA, Wilson SH. Using human primary foreskin fibroblasts to study cellular damage and mitochondrial dysfunction. Current Protocols in Toxicology 2020; 86(1): e99. https://doi.org/10.1002/cptx.99

[32] Souren NY, Fusenig NE, Heck S, Dirks WG, Capes-Davis A, Bianchini F, *et al*. Cell line authentication: a necessity for reproducible biomedical research. The EMBO Journal 2022; 41(14): e111307. https://doi.org/10.15252/embj.2022111307

[33] Yasin Al-Samarray YS, Jumaa AH, Hashim WS, Khudhair YI. The cytotoxic effect of ethanolic extract of cnicus Benedictus L. flowers on the murine mammary adenocarcinoma Cancer cell line AMN-3. Biochemical & Cellular Archives 2020; 20.

[34] Le Berre M, Gerlach JQ, Dziembała I, Kilcoyne M. Calculating half maximal inhibitory concentration (IC 50) values from glycomics microarray data using graphpad prism. Glycan Microarrays: Methods and Protocols 2022: 89-111.
https://doi.org/10.1007/978-1-0716-2148-6_6

[35] He Y, Zhu Q, Chen M, Huang Q, Wang W, Li Q, *et al*. The changing 50% inhibitory concentration (IC50) of cisplatin: a pilot study on the artifacts of the MTT assay and the precise measurement of density-dependent chemoresistance in ovarian cancer. Oncotarget 2016; 7(43): 70803.
https://doi.org/10.18632/oncotarget.12223

[36] Bezerra JN, Gomez MCV, Rolón M, Coronel C, Almeida-Bezerra JW, Fidelis KR, *et al*. Chemical composition, Evaluation of Antiparasitary and Cytotoxic Activity of the essential oil of Psidium brownianum MART EX. DC. Biocatalysis and Agricultural Biotechnology 2022; 39: 102247.
https://doi.org/10.1016/j.bcab.2021.102247

[37] Meyer CT, Wooten DJ, Lopez CF, Quaranta V. Charting the Fragmented Landscape of Drug Synergy. Trends Pharmacol Sci 2020; 41(4): 266-80.
https://doi.org/10.1016/j.tips.2020.01.011

[38] Chou T-CJS. The combination index (CI< 1) as the definition of synergism and of synergy claims. Elsevier; 2018; pp. 49-50.
https://doi.org/10.1016/j.synres.2018.04.001

[39] Tokarska-Schlattner M, Zeaiter N, Cunin V, Attia S, Meunier C, Kay L, *et al*. Multi-method quantification of acetyl-coenzyme A and further acyl-coenzyme A species in normal and ischemic rat liver. International Journal of Molecular Sciences 2023; 24(19): 14957.
https://doi.org/10.3390/ijms241914957

[40] Duan Y, Liu J, Li A, Liu C, Shu G, Yin G. The Role of the CPT Family in Cancer: Searching for New Therapeutic Strategies. Biology 2024; 13(11): 892.
https://doi.org/10.3390/biology13110892

[41] Yuki K. Phosphoribosyl pyrophosphate amidotransferase: A novel biomarker and therapeutic target for nasopharyngeal carcinoma: Kanazawa University.

[42] Salentin S, Schreiber S, Haupt VJ, Adasme MF, Schroeder MJNar. PLIP: fully automated protein–ligand interaction profiler 2015; 43(W1): W443-W7.
https://doi.org/10.1093/nar/gkv315

[43] Chen G, Seukep AJ, Guo MJMd. Recent advances in molecular docking for the research and discovery of potential marine drugs 2020; 18(11): 545.
https://doi.org/10.3390/md18110545

[44] Rahayu NI, Muktiarni M, Hidayat Y. An application of statistical testing: A guide to basic parametric statistics in educational research using SPSS. ASEAN Journal of Science and Engineering 2024; 4(3): 569-82.
https://doi.org/10.17509/ajse.v4i3.76092

[45] Mahdi HM, Wadee SA. Interaction Effect of Methotrexate and Aspirin on MCF7 cell line Proliferation: In vitro Study. Journal of Advanced Veterinary Research 2023; 13(9): 1767-71.

[46] Guo L-Y, Xing X, Tong J-B, Li P, Ren L, An C-X. Qsar Aided Design of Potent Ret Inhibitors Using Molecular Docking, Molecular Dynamics Simulation and Binding Free Energy Calculation. Molecular Dynamics Simulation and Binding Free Energy Calculation 2024.
https://doi.org/10.2139/ssrn.4886845

[47] Liang K. Mitochondrial CPT1A: Insights into structure, function, and basis for drug development. Frontiers in Pharmacology 2023; 14: 1160440.
https://doi.org/10.3389/fphar.2023.1160440

[48] Dutka M, Bobiński R, Francuz T, Garczorz W, Zimmer K, Ilczak T, *et al*. SGLT-2 inhibitors in cancer treatment—mechanisms of action and emerging new perspectives. Cancers 2022; 14(23): 5811.
https://doi.org/10.3390/cancers14235811

[49] Zhou J, Zhu J, Yu S-J, Ma H-L, Chen J, Ding X-F, *et al*. Sodium-glucose co-transporter-2 (SGLT-2) inhibition reduces glucose uptake to induce breast cancer cell growth arrest through AMPK/mTOR pathway. Biomedicine & Pharmacotherapy 2020; 132: 110821.
https://doi.org/10.1016/j.biopha.2020.110821

[50] Basak D, Gamez D, Deb S. SGLT2 inhibitors as potential anticancer agents. Biomedicines 2023; 11(7): 1867.
https://doi.org/10.3390/biomedicines11071867

[51] Hashim WS, Yasin YS, Jumaa AH, Al-Zuhairi MI, Abdulkareem AH. Physiological Scrutiny to Appraise a Flavonol Versus Statins. Biomedical and Pharmacology Journal 2023; 16(1): 289-93.
https://doi.org/10.13005/bpj/2610

[52] Jarad A. Diabetic Wound Healing Enhancement by Tadalafil. International Journal of Pharmaceutical Research 2020; 12(03).
https://doi.org/10.31838/ijpr/2020.12.03.121

[53] Said AM, Numan IT, Hamad MN. Study of the cytotoxic and genotoxic effects for fractioniated extracts of convolulus arvensis on bone marrow in mice. International Journal of Pharmacy and Pharmaceutical Sciences Received 2013; 18: 303-5.

[54] Trefely S, Huber K, Liu J, Noji M, Stransky S, Singh J, *et al*. Quantitative subcellular acyl-CoA analysis reveals distinct nuclear metabolism and isoleucine-dependent histone propionylation. Molecular Cell 2022; 82(2): 447-62. e6.
https://doi.org/10.1016/j.molcel.2021.11.006

[55] Xie J, Yu Z, Zhu Y, Zheng M, Zhu Y. Functions of coenzyme A and acyl-CoA in post-translational modification and human disease. Frontiers in Bioscience-Landmark 2024; 29(9): 331.
https://doi.org/10.31083/j.fbl2909331

[56] Salentin S, Schreiber S, Haupt VJ, Adasme MF, Schroeder M. PLIP: fully automated protein–ligand interaction profiler. Nucleic Acids Research 2015; 43(W1): W443-W7.
https://doi.org/10.1093/nar/gkv315

[57] Chen G, Seukep AJ, Guo M. Recent advances in molecular docking for the research and discovery of potential marine drugs. Marine Drugs 2020; 18(11): 545.
https://doi.org/10.3390/md18110545

Received on 27-11-2025 Accepted on 25-12-2025 Published on 31-12-2025

https://doi.org/10.30683/1929-2279.2025.14.26